International Journal of Thin Film Science and Technology

Volume 10
Issue 3 *Sep. 2021*

Article 9

2021

Influence of Doping Concentration on the Properties of Tin Doped Zinc Oxide Thin Films Prepared by Spray Pyrolysis for Photovoltaic Applications

K. Salim
Laboratoire d'Elaboration et de Caractérisation des Matériaux, département d'électronique, Université Djilali Liabes, BP89, Sidi Bel Abbés 22000. Algeria, karim22000@hotmail.com

M. N. Amroun
Laboratoire d'Elaboration et de Caractérisation des Matériaux, département d'électronique, Université Djilali Liabes, BP89, Sidi Bel Abbés 22000. Algeria, karim22000@hotmail.com

W. Azzaoui
Laboratoire d'Elaboration et de Caractérisation des Matériaux, département d'électronique, Université Djilali Liabes, BP89, Sidi Bel Abbés 22000. Algeria, karim22000@hotmail.com

International Journal of Thin Films Science and Technology

http://dx.doi.org/10.18576/ijtfst/100309

Influence of Doping Concentration on the Properties of Tin Doped Zinc Oxide Thin Films Prepared by Spray Pyrolysis for Photovoltaic Applications

K. Salim[*], *M. N. Amroun* and W. Azzaoui

Laboratoire d'Elaboration et de Caractérisation des Matériaux, département d'électronique, Université Djilali Liabes, BP89, Sidi Bel Abbés 22000. Algeria

Received: 21 May 2021, Revised: 22 Jun. 2021, Accepted: 24 Jul. 2021.
Published online: 1 Sep. 2021.

Abstract: This work reports on the preparation and characterization of zinc oxide (ZnO) thin films by spray pyrolysis on glass substrates. The effect of Sn doping with 1% Sn (TZO-1.00), 1.5% Sn (TZO-1.50), 2% Sn (TZO-2.00) on the structural, optical and electrical properties of the obtained films was studied. The obtained films are characterized by different techniques such as X-ray diffraction (XRD), UV-visible and electrical Hall Effect measurements. The results of the XRD characterization indicate that all the films have the polycrystalline hexagonal wurtzite structure with a preferred orientation (002). Spectroscopic measurements in the UV-VIS-IR wavelength range were found to give good average transmittance values of about 70%, with a high transmittance of 75% with 1.5% Sn doping. The optical gap value increases in the range of 3.23 to 3.29 eV with increasing tin content. The electrical analysis shows that the conductivity improves slightly with doping compared to the pure ZnO film.

Keywords: ZnO, thin films, spray pyrolysis Solar Cells,.

1 Introduction

Zinc oxide (ZnO) has become a widely followed TCO by researchers in recent years due to its optical and electronic properties [1]. ZnO is an n-type semiconductor with large exciton energy of 60 meV [2] and a large direct band gap of 3.34 eV [3,4]. Pure ZnO thin films have low transmittance and electrical conductivity compared to doped films, which is due to their low carrier density. In order to improve its physical properties, ZnO has to be doped with different elements such as Sn, Al, F, Ge, Ti, Bi, Cu etc. [5].
Transparent conductive oxide thin films have been applied in several fields like as, solar cells [4], UV photo-detectors and piezoelectric transducers [3], gas detectors [5]. Several methods such as; successive ionic layer adsorption [1], chemical route [7], pulsed laser [8], and spray pyrolysis [2] have been used for the deposited of zinc oxide films.
In this work, the effect of tin (Sn) doping on the optical and electrical properties of ZnO thin films produced by the spray pyrolysis technique was studied.

2 Experimental Details

ZnO films were prepared by the spray pyrolysis technique at different doping concentrations. In the first step, the sputtering solution was prepared using zinc nitrate (Zn (NO3)2,6H2O) (0.1 M) as a precursor in 50 ml of doubly distilled water. After stirring at room temperature, an amount of tin chloride (SnCl2.2H2O) with different ratio was added (1% Sn: TZO-1.00, 1.5% Sn: TZO-1.50, 2% Sn: TZO-2.00). The solution mixture was stirred to give a clear solution at the end. The substrate temperature was set at 350±10°C, and the solution was introduced into a spray nozzle at a constant atomization pressure. The solution flow rate was 2 ml/min. The distance between the nozzle and the substrate was 30 cm. The values of the thickness are 291, 278, 295 and 283 nm for ZnO, TZO-1.00, and TZO-1.50 and TZO-2.00 films, respectively.

Structural characterization was performed at room temperature using a Bruker D2 Phaser X- ray diffractometer with CuKα radiation (λ = 1.5406 Å). The XPS measurements were carried out on a Kratos Axis Ultra using Al Kα (1486.6 eV) radiation. High resolution spectra were acquired at 20 eV pass energy with energy resolution of 0.9 eV. Transmittance spectra were recorded between 200 and 2500 nm wavelength using a dual beam UV-vis-NIR spectrophotometer type JASCO 570. The chemical composition of the deposited films was studied by EDS analysis using a Jeol scanning electron microscope, model

[*]Corresponding author E-mail: karim22000@hotmail.com

JSM-5800, equipped with an energy dispersive X- ray detector. Electrical parameters were measured using the ECOPIA HMS-5000 Hall effect measurement system at room temperature.

3 Results and Discussion

3.1Structural and morphological characterization

X-ray diffraction (XRD) spectra of undoped and Sn-doped ZnO thin films with different concentrations illustrated in Figure.1.a.The presence of several peaks indicating the polycrystalline nature of the obtained films. All the peaks observed in these spectra correspond to the wurtzite structure of ZnO according to the comparison with JCPDS map No. 36-1451 [6]. No peaks corresponding to other phases such as tin, tin oxide or other tin compounds were detected in these XRD spectra; this shows the good incorporation of Sn atoms in the ZnO matrix and therefore the success of the doping. The obtained TZO-1.5 and TZO-2.00 thin films are composed of crystallites having orientations along several crystallographic planes with a preferred orientation along [002]. Furthermore, the obtained TZO-1.00 and ZnO films are strongly oriented along [002] of the c-axis perpendent to the substrate. This result indicates that the incorporation of the Sn atom in the ZnO matrix does not modify the preferential growth.

To determine the crystallite size (D) of the films, the Scherer formula [7,8] (Eq.1) is used, which uses the measurement of the width at half maximum of the diffraction peaks β (FWHM).

$$D = \frac{0.9\lambda}{\beta cos\theta} \quad (1)$$

With:

D: the size of the crystallites in Å;

β : the width at half height expressed in radians;

θ: the angular position of the diffraction peak under consideration.

The dislocation density (δ) is estimated by the following relationship [9]:

$$\delta = \frac{1}{D^2} \quad (2)$$

The strain values (ε) of the ZnO film along the (002) planes were calculated using the following formula [10]:

$$\varepsilon = \frac{\beta cos\theta}{4} \quad (3)$$

Examination of the results reported in table 1 indicates that the degree of preferential orientation decreases progressively with increasing doping. Indeed, with the doping, the width at half maximum (FWHM) of the (002) peak increases with the increase of the Sn content.

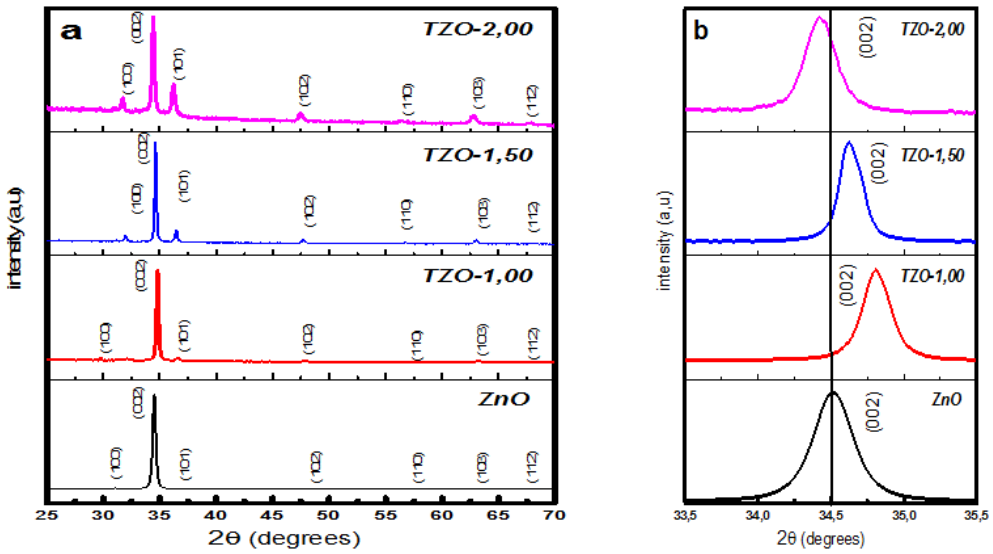

Figure 1: (a) XRD spectra of ZnO and Sn-doped ZnO thin films with different concentrations. (b)Magnified spectra of the peak related to the [002] plane.

Table 1: Structural parameters of ZnO and Sn-doped ZnO thin films with different concentrations.

Samples	2θ0 (002)	FWHM $.10^{-3}$ (°)	Crystal size (nm)	a (Å)	c (Å)	(ε) deformation (10^{-4})	(δ) dislocation density (10^{-4} Line/nm^2)
ZnO	34.52	5.09	28.50	3.241	5.192	12.15	12.3
TZO-1.00	34.79	5.54	25.61	3.240	5.188	13.20	14.2
TZO-1.50	34.63	5.67	23.78	3.239	5.184	13.92	14.9
TZO-2.00	34.44	5.93	21.24	3.240	5.187	14.24	15.3

Moreover, we notice that the sizes of the crystallites oriented along the [002] crystallographic plane decrease with doping, these evolutions indicate that Sn doping deteriorates the crystallinity of ZnO thin films, which has already been reported on the work of M. Vasanthi et al. [11]. On the other hand, the small shift of the (002) peak (fig.1.b) in its angular position indicates some residual stress inside the Sn-doped films. Jeong et al [12] observed a similar shift to large values of 2θ in the position of the (002) peak with increasing Sn doping, which can be attributed to residual stress in the ZnO thin films caused by the difference in ionic size between Zn^{2+} (0.74Å) and Sn^{+4} (0.69Å). Similar behaviors have already been observed in several works [12,14].

The Figure.2 illustrate the general (XPS) spectrum of the ZnO doped 1% Sn thin film, the Zinc, Oxygen and Tin peaks are presented. Illustrates the high resolution of Zn2p, O1s and Sn3d in the figure 3(a,b,c) respectively, the Zn2p spectrum (Fig.3.a) shows two peaks located at 1021.09 eV and 1044.19 eV with a splitting energy (Δ) of 23.12 eV and are attributed to Zn 2p3/2 and Zn 2p1/2 respectively for a chemical state of Zn^{2+} in ZnO [15]. The O1 spectrum (Fig.3.b) can be decomposed into two peaks, the more intense one is located at 529.91 eV and assigned to the Zn-O bond in the wurtzite structure ZnO, the peak at 531.19 eV could be associated with oxygen vacancies in the deficient regions of the ZnO matrix [16] or with adsorbed oxygenated impurities [17].

The figure 3.c shows the spectrum of Sn 3d. The binding energy of the Sn 3d5/2 peak located at 486.19 eV indicates the Sn^{4+} chemical state which is in good agreement with the results reported in the literature [18].

The Figure.4.a and 4.b shows the presence of peaks of the chemical elements zinc, oxygen and tin. No other peaks related to other chemical elements, were observed, which confirms the (XPS) analysis. Furthermore, the presence of silicon on all samples is attributed to the glass substrate. Quantitative analysis of the chemical elements that make up the TZO-1.00 and TZO-2.00 thin films, notably tin, gives a percentage value of this element in line with the desired doping levels (1% and 2%).

3.2. *Optical characterization*

The optical transmission spectra of ZnO, TZO-1.00, TZO-1.50 and TZO-2.00 thin films are presented in Figure 5. The optical transparency of the films is clearly increased with Sn doping. Indeed, the transmittances increase from 65% of undoped ZnO film to 75% TZO-1.50 thin film with an increase of about 10%. This improvement in optical transparency can be explained by the reduction in the surface roughness of the films with Sn incorporation [13].

The value of the optical band gap energy of all samples was calculated; we used the Tauc relation [20]. This was done by plotting (αhυ)2 as a function of the photon energy hυ according to equation (4) :

$$(ahv)^n = A(hv - Eg) \quad (4)$$

Where α is the absorption coefficient, hv the photon energy, A constant and Eg the optical band gap. We take n=2 for direct band gap semiconductors.

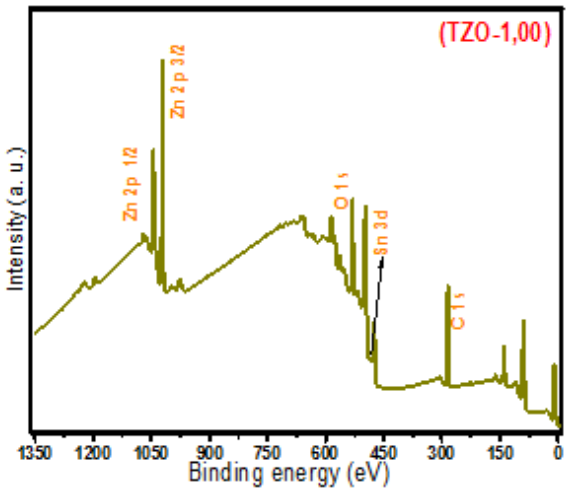

Figure 2: XPS analysis spectrum: (a) the Zn2p peak, (c) the O1s peak and (c) the Sn3d peak.

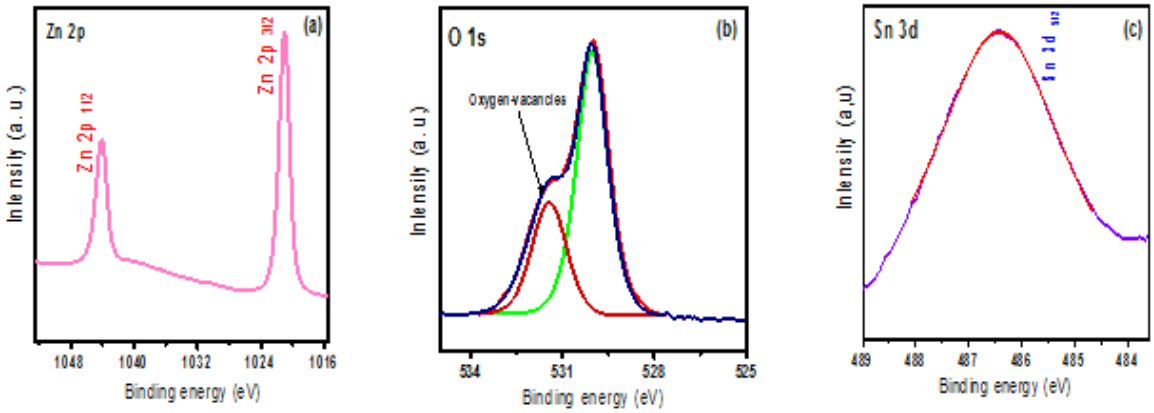

Figure 3: XPS analysis spectrum: (a) the Zn2p peak, (c) the O1s peak and (c) the Sn3d peak.

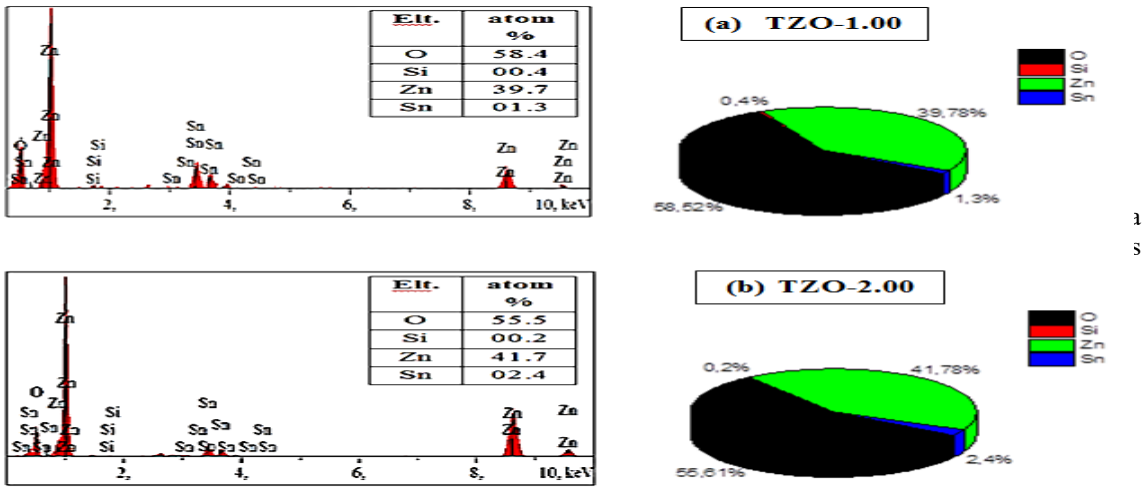

Figure 4: EDS spectra of thi

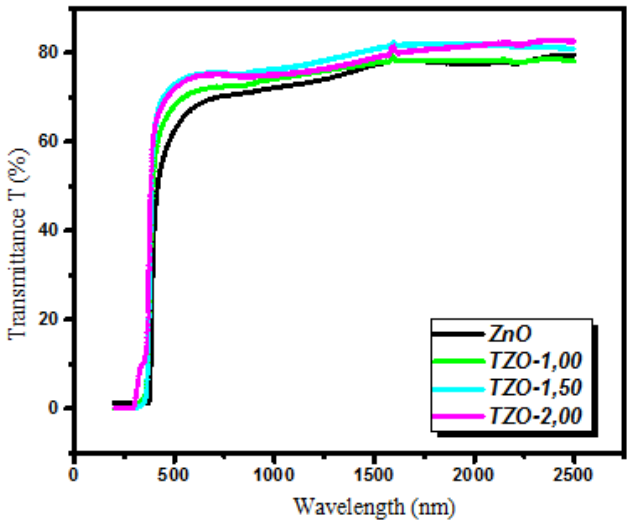

Figure 5: Optical transmittance spectra of ZnO and Sn-doped ZnO thin films with different concentrations.

The optical gap increased from 3.23 eV for undoped ZnO films to 3.29 eV for 1.5% Sn doped ZnO films, this increase in the band gap can be explained by the contribution Burstein-Moss effect [21]. Moreover, the doping creates degenerate energy levels that push the Fermi level to move above the conduction band edge. This effect induces an increase in the band gap [4, 21].
In order to estimate the disorder in the thin films, we used the Urbach energy. The Urbach energy (Eu) of the samples was calculated using following equation [19, 20]:

$$\alpha = \alpha_0 \exp(\frac{h\nu}{E_U}) \quad (5)$$

Where E_U is the Urbach energy, α is the absorption coefficient and α_0 is a constant.

Table 2: Urbach energy of ZnO and Sn-doped ZnO thin films with different concentrations.

Samples	Urbach energy (Eu) (eV)
ZnO	0.09
TZO-1.00	0.12
TZO-1.50	0.13
TZO-2.00	0.14

The Urbach energy values of pure and doped ZnO films are presented in Table 2. The increase in Urbach energy (disorder) with Sn incorporation is probably due to the degradation of the structural quality of the layers [23], which confirm the results obtained by XRD data.

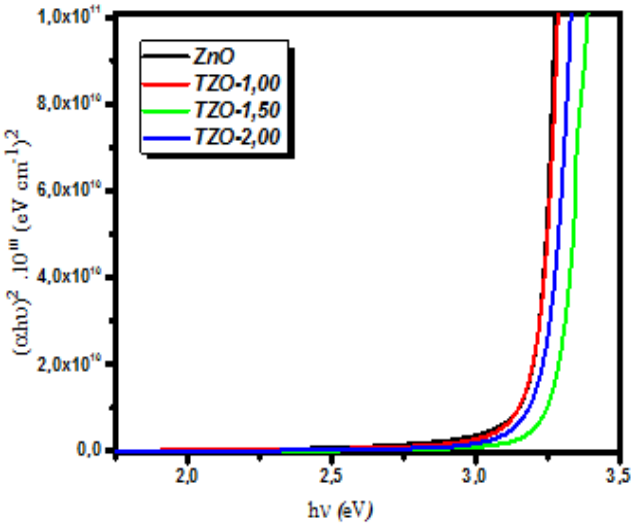

Figure 6: Variation of (αhν)2 as a function of hυ of ZnO and Sn-doped ZnO thin films with different concentrations.

The refractive index (n), extinction coefficient (k) and the thickness (d) of the thin films were estimated with the spPS (seed preprocessing Pattern search) technique [24].

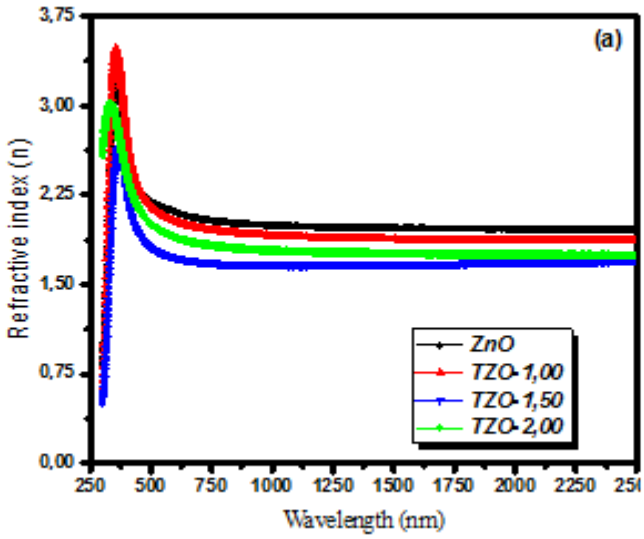

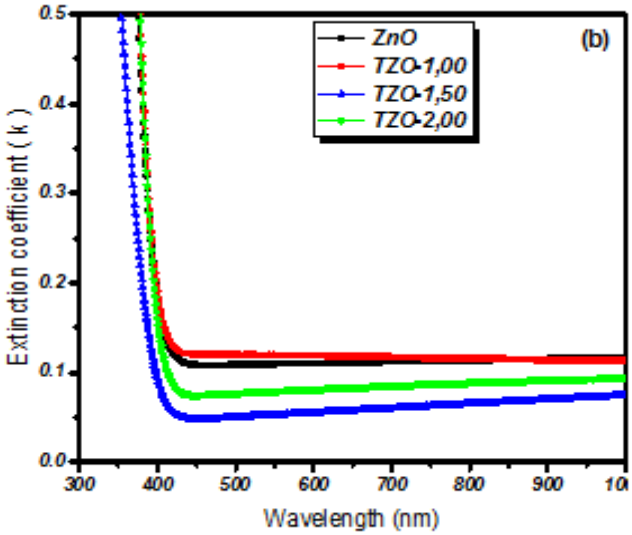

Figure 7: The refractive index (a), extinction coefficient (b)

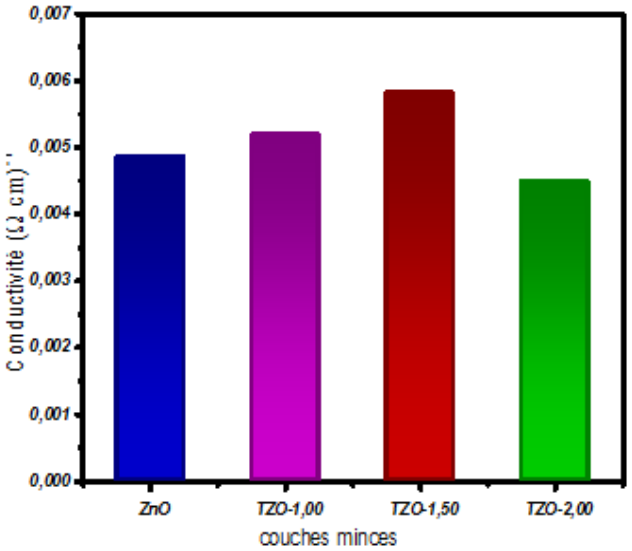

Figure 8: Evolution of the electrical conductivity of ZnO and Sn-doped ZnO thin films with different concentrations.

The refractive index (n) and extinction coefficient (k) decrease from 2.14 to 1.76 and 0.12 to 0.05 respectively with Sn doping in the visible wavelength range, which may be could attributed to the decrease in the roughness of the films, a similar result observed by N. Chahmat et al [25]. These films with low values of n and k are recommended for optoelectronic device applications such as solar cell window layers [26].

3.3 Electrical properties

Hall Effect of the ZnO, TZO-1.00, TZO 1.50 and TZO-2.00 were studied at room temperature using the ECOPIA HMS-5000 Hall effect measuring system. Table 3 summarized the electrical parameters, i.e. conductivity, mobility and carrier concentration for the samples.

The negative values of the carrier concentrations show that the deposited films are n-type. It can be seen from this table that the order of magnitude improves slightly for all values of the conductivity of ZnO and Sn-doped ZnO thin films with different concentrations with a slight increase in the carrier concentration. This result means that the doping of ZnO thin films with low tin content does not have a very effective impact on their electrical properties (Fig.8).
This result is in line with what was reported by Chien-Yie Tsay et al [23] in which the authors found a slight change in resistivity at low Sn doping levels (1-2%), and a decrease in the concentration of charge carriers due to grain boundary traps at high Sn doping levels above 2%

Table 3: Electrical parameters of ZnO and Sn-doped ZnO thin films with different concentrations.

Samples	Mobility (cm^2/Vs)	Carrier concentrations (cm^{-3})	Conductivity $(\Omega .cm)^{-1}$
ZnO	$4.30.10^{-01}$	$-5.9.10^{+16}$	4.10^{-03}
TZO-1.00	$4.32.10^{-01}$	$-9.7.10^{+16}$	5.10^{-03}
TZO-1.50	$4.35.10^{-01}$	$-1.3.10^{+16}$	6.10^{-03}
TZO-2.00	4.43.10-01	$-0.3.10^{+16}$	3.10^{-03}

4. Conclusion

In this work, a study of the structural, optical and electrical properties of undoped and Sn- doped ZnO thin films with different concentrations was carried out. The aim of this contribution is to see the effect of tin incorporation in the ZnO lattice as transparent conducting oxides in solar cells. The XRD analysis confirmed that the deposited films have a hexagonal wurtzite structure with a preferred orientation of (002) and that no impurity phase was observed. The crystallite sizes are calculated using the scherrer formula, which shows that the doped ZnO layers have the smallest crystallite size. UV-visible analysis showed that all layers have high transparency with an average transmission value of about 70% before doping and rising to 75% after doping, the highest band gap value was obtained for the doped layer (TZO-1.5). Electrical measurements were also carried out giving a maximum electrical conductivity of the order of 6.10^{-03} (Ω.cm)-1 for the thin film (TZO-1.5). This suggests that the deposited Sn doped ZnO thin films are a good candidate for optoelectronic applications such as photovoltaic solar cells.

References

[1] Ranran Fan, Fei Lu, Kaikai Li, Single-mode channel waveguide at 1540 nm in Er-doped ZnO thin film, J. Lumin. **192** ,(410–413),2017.

[2] A. Ouhaibi, M.Ghamnia, M.A.Dahamni, V.Heresanu, C. Fauquet, D. Tonneau, The effect of strontium doping on structural and morphological properties of ZnO nanofilms synthesized by ultrasonic spray pyrolysis method, J. Sci. Adv. Mater. Devices **3**,(29-36),2018

[3] Anotti, C.G. Van de Walle, Fundamentals of zinc oxide as a semiconductor, Reports on Progress in Physics **72** (126501-126529) 2009.

[4] F.Z. Bedia, A. Bedia, N. Maloufi, M. Aillerie, F. Genty, B. Benyoucef, Effect of tin doping on optical properties of nanostructured ZnO thin films grown by spray pyrolysis technique, Journal of Alloys and Compounds **616** ,(312-318), 2014.

[5] H. Liu, V. Avrutin, N. Izyumskaya, Ü. Özgür, H. Morkoç, Transparent conducting oxides for electrode applications in light emitting and absorbing devices, Superlattices and Microstructures **48**,(458-484),2010.

[6] Joint Committee on Powder Diffraction Standards Powder Diffraction File. 1988 International Center for Diffraction Swarthmore PA (card 36-1451).

[7] Adel Taabiuche, Contribution à l'étude structurale et microstructurale de films ZnO obtenus par ablation laser, thèse de Doctorat, Université Mentouri de Constantine, Algérie (2010).

[8] Belkacemi Hamida, Dépôt et Caractéri sat ions des Couches minces de ZnO Avec Di f férentes Sources de Zinc, thèse de Doctorat, Université de Mohamed khider de Biskra, Algérie (2011).

[9] M. N. Amroun, K. Salim, A. H. Kacha and M. Khadraoui, Tco's Thin Films Grown By Spray Pyrolysis Technique For Window Layer Of Solar Cell Application: A Comparative Study, Int. J. Thin.Film. Sci. Tec. **9**, No. 2, (103-110), 2020.

[10] M. N. Amroun, K. Salim, A. H. Kacha, Molarities Effect on Structural Optical and Electrical Properties of Nanostructured Zinc Oxide deposited by Spray Pyrolysis Technique, Int. J. Thin. Fil. Sci. Tec. 10, No. **1**, (67-73) ,2021.

[11] M. Vasanthi, K. Ravichandran, N. Jabena Begum, G. Muruganantham, S. Snega, A. Panneerselvam, P. Kavitha, Influence of Sn doping level on antibacterial activity and certain physical properties of ZnO films deposited using a simplified spray pyrolysis technique, Superlattices and Microstructures **55** , (180-190) ,2013.

[12] J. H. Lee, B. O. Park, Transparent conducting ZnO: Al, In and Sn thin films deposited by the sol–gel method, Thin Solid Films **42,(**694),2003.

[13] K. Salim, M. Medles, A. Nakrela, R. Miloua, A. Bouzidi, R. Desfeux, Enhancement of optical and electrical properties of spray pyrolysed ZnO thin films obtained from nitrate chemical by Al-Sn co-doping, Optik - International Journal for Light and Electron Optics **210** ,(164504),2020.

[14] A. Karthick, G. Umadevi, D. Pradhabhan, Structural, optical and antibacterial activity studies of sn doped zno thin films prepared by chemical spray pyrolysis technique, Int. J. Res. Anal. Rev. **5** ,(246-260),2018.

[15] A. Amala Rani, Suhashini Ernest, Structural, morphological, optical and compositional characterization of spray deposited Ga doped ZnO thin film for desensitized solar cell application, Superlattices Microstructure **75** (398-408),2014.

[16] G. H. Zhang, P. Y. Wang, X. Y. Deng, Y. Chen, D. J. Gengzang, X. L. Wang, W. J. Chen , CTAB-assisted synthesis of 3D SN doped ZnO nanostructures with enhanced acetone sensing performance, Materials Letters **162** ,(265-268),2015.

[17] Zhixiang Ye, Ting Wang, Shuang Wu, Xiaohong Ji, Qinyuan Zhanga, Na-doped ZnO nanorods fabricated by chemical vapor deposition and their optoelectrical properties, J. Alloys. Compd. **690** ,(189-194),2017.

[18] G. Turgut, E. Sönmez, A study of Pb-Doping effect on structural, optical, and morphological properties of ZnO thin films deposited by sol–gel spin coating, Metall,a Mater. Trans. A **45** ,(3675-3685),2014.

[19] H. Aydin, H. M. El-Nasser, C. Aydin Ahmed, A. Al-Ghamdi, F. Yakuphano glu, Synthesis and characterization of nanostructured un-doped and Sn doped ZnO Thin Films via Sol–Gel Approach, App. Surf. Sci. **350,**(109-114),2015.

[20] W. Daranfed, M.S. Aida, A. Hafdallah, H. Lekiket , Substrate temperature in- fluence on ZnS thin films prepared by ultrasonic spray, Thin Solid Films **518** ,(1082–1084),2009 .

[21] N. Rajeswari Yogamalar, A. Chandra Bose, Burstein–Moss shift and room temperature near-band-edge luminescence in lithium-doped zinc oxide, Appl. Phys. A **103,** (33-42)2013.

[22] Anuj Kumar, Sol gel synthesis of zinc oxide nanoparticles and their application as nano-composite electrode material for super capacitor, Journal of Molecular Structure **15**, (128654), 2020.

[23] Chien Yie Tsay, Hua-Chi Cheng, Yen-Ting Tung, Wei Hsing Tuan, Chung Kwei Lin, Effect of Sn-doped on microstructural and optical properties of ZnO thin films

deposited by sol–gel method, Thin Solid Films **517** **(**1032-1036) ,2008.

[24] R. Miloua, Z. Kebbab, F. Chiker, K. Sahraoui, M. Khadraoui, N. Benramdane, Determination of layer thickness and optical onstants of thin films by using a modified pattern search method, Opt. Lett. **37** ,(449-451), 2012.

[25] N. Chahmat, T. Souier, A. Mokri, M. Bououdina, M. Aida, M. Ghers, Structure, microstructure and optical properties of Sn-doped ZnO thin films, J. Alloys Compd.,**593**,(148-153), 2014.

[26] M. Miki-Yoshida, J. Morales, J. Solis, Influence of Al, In, Cu, Fe and Sn dopants on the response of thin film ZnO gas sensor to ethanol vapour, Thin Solid Films, **373** (137-140),2000.